Environmental drivers of spatial variation in whole-tree transpiration in an aspen-dominated upland-to-wetland forest gradient

Michael M. Loranty,[1] D. Scott Mackay,[1] Brent E. Ewers,[2] Jonathan D. Adelman,[2] and Eric L. Kruger[3]

Received 16 June 2007; revised 22 October 2007; accepted 9 November 2007; published 29 February 2008.

[1] Assumed representative center-of-stand measurements are typical inputs to models that scale forest transpiration to stand and regional extents. These inputs do not consider gradients in transpiration at stand boundaries or along moisture gradients and therefore potentially bias the large-scale estimates. We measured half-hourly sap flux (J_S) for 173 trees in a spatially explicit cyclic sampling design across a topographically controlled gradient between a forested wetland and upland forest in northern Wisconsin. Our analyses focused on three dominant species in the site: quaking aspen (*Populus tremuloides* Michx), speckled alder (*Alnus incana* (DuRoi) Spreng), and white cedar (*Thuja occidentalis* L.). Sapwood area (A_S) was used to scale J_S to whole tree transpiration (E_C). Because spatial patterns imply underlying processes, geostatistical analyses were employed to quantify patterns of spatial autocorrelation across the site. A simple Jarvis type model parameterized using a Monte Carlo sampling approach was used to simulate E_C (E_{C-SIM}). E_{C-SIM} was compared with observed E_C (E_{C-OBS}) and found to reproduce both the temporal trends and spatial variance of canopy transpiration. E_{C-SIM} was then used to examine spatial autocorrelation as a function of environmental drivers. We found no spatial autocorrelation in J_S across the gradient from forested wetland to forested upland. E_C was spatially autocorrelated and this was attributed to spatial variation in A_S which suggests species spatial patterns are important for understanding spatial estimates of transpiration. However, the range of autocorrelation in E_{C-SIM} decreased linearly with increasing vapor pressure deficit, implying that consideration of spatial variation in the sensitivity of canopy stomatal conductance to D is also key to accurately scaling up transpiration in space.

Citation: Loranty, M. M., D. S. Mackay, B. E. Ewers, J. D. Adelman, and E. L. Kruger (2008), Environmental drivers of spatial variation in whole-tree transpiration in an aspen-dominated upland-to-wetland forest gradient, *Water Resour. Res.*, *44*, W02441, doi:10.1029/2007WR006272.

1. Introduction

[2] Hydrologic studies utilizing estimates of forest canopy transpiration or evapotranspiration typically use a mean observed species sap flux value and an estimate of sapwood area per unit ground area to scale to the stand level [*Cermak et al.*, 1995; *Ewers et al.*, 2002; *Hatton et al.*, 1995; *Oren et al.*, 1998; *Santiago et al.*, 2000]. Such an approach assumes that transpiration per tree is spatially well mixed at the stand level, an assumption that has not been explicitly tested. Hydrologic models operating at catchment, regional, and global scales all typically incorporate transpiration estimates [*Band*, 1993; *Band and Moore*, 1995; *Famiglietti and Wood*, 1994; *Foley et al.*, 1996, 2000; *Gedney et al.*, 2006; *Running and Coughlan*, 1988; *Sellers et al.*, 1997; *Wigmosta et al.*, 1994], and the implications of spatially varying transpiration are particularly pertinent for catchment scale models [*Seyfried and Wilcox*, 1995]. Advances in model sophistication and incorporation of spatial heterogeneity into hydrologic models has resulted in a demand for complementary spatial data [*Grayson et al.*, 2002].

[3] Advances in statistical methods designed for dealing with spatial data have drawn increased attention to the role of spatial heterogeneity in ecosystem function [*Legendre*, 1993]. Spatial autocorrelation in areas considered to be environmental gradients are particularly important in this context. Recognizing this functional heterogeneity inherently suggests that it should be included in ecosystem and hydrologic models [*Legendre*, 1993; *Legendre and Legendre*, 1998]. In the present study we characterize spatial variation in transpiration per tree in forest stands with the ultimate goal of identifying the underlying mechanisms and incorporating this into a hydrologic model used to estimate transpiration.

[1]Department of Geography, State University of New York at Buffalo, Buffalo, New York, USA.
[2]Department of Botany, University of Wyoming, Laramie, Wyoming, USA.
[3]Department of Forest and Wildlife Ecology, University of Wisconsin–Madison, Madison, Wisconsin, USA.

0043-1397/08/2007WR006272

[4] Transpiration per unit xylem area (J_S) and transpiration per tree (E_C), are regulated by a number of biological and environmental variables. It is reasonable to expect some if not all of these variables to vary in space at the stand level. As such, J_S, and E_C may also be expected to vary spatially as well. A number of studies have reported an observed decrease in J_S, and/or E_C as a result of declines in soil moisture for a variety of species [*Gazal et al.*, 2006; *Lagergren and Lindroth*, 2002; *Oren and Pataki*, 2001; *Pataki et al.*, 2000]. Although these observations deal primarily with temporal variation in soil moisture, J_S and E_C spatial heterogeneity could be expected as well [*Katul et al.*, 1997], particularly during periods of drought [*Granier et al.*, 2000]. Additional heterogeneity in soil moisture attributable to topography, soil composition, and soil depth has also been shown to cause spatial variation in E_C particularly during transitions between wet and dry periods [*Granier et al.*, 2000; *Tromp-van Meerveld and McDonnell*, 2006]. Biological differences within and between species can also underlie variations in J_S, and E_C. Changes in J_S with stem diameter have been reported in the literature [*Oren et al.*, 1999]. Declines of J_S with age, sapwood area (A_S) and height attributed to lower hydraulic conductance (K_S) have been observed in several species [*Alsheimer et al.*, 1998; *Hubbard et al.*, 1999; *Lundblad and Lindroth*, 2002; *Schafer et al.*, 2000; *Wullschleger and King*, 2000]. In addition to spatial variation, short-term (i.e., diurnal) temporal variation in J_S, and E_C may be expected because of the relationship between stomatal conductance (G_S) and sensitivity to vapor pressure deficit (D) [*Ewers et al.*, 2007b].

[5] Our aim in this study is to explore spatial variation in J_S and E_C across a moisture gradient between a forested upland and a forested wetland using a combination of field and simulation techniques. To achieve this we employed approximately 173 heat dissipation sap flux sensors [*Granier*, 1987] in northern Wisconsin and used observed values for model parameterization. Geostatistical analysis techniques have become increasingly prevalent in hydrology and ecosystem studies [*Gallardo and Covelo*, 2005; *Grayson et al.*, 2002; *Western et al.*, 2004] and we have employed these tools to characterize spatial patterns across the site. Simulated E_C values were used to analyze temporal trends in spatial autocorrelation as gaps in the observed data prevented robust spatial analyses. We tested the following four hypotheses using both observed and simulated data where applicable: (1) J_S is spatially autocorrelated across a moisture gradient from a forested wetland to forested upland; (2) E_C is spatially autocorrelated across a moisture gradient from a forested wetland to forested upland; (3) patterns of spatial autocorrelation in E_C are driven by environmental variables and so they can be simulated using a simple Jarvis model (equation (3), see below); and (4) patterns of spatial autocorrelation in a) J_S and b) E_C vary temporally with D.

2. Methods

2.1. Site Description

[6] The study was conducted in northern Wisconsin, near Park Falls (45.9458°N, 90.2723°W). The study site was situated less than 1 km southeast of the WLEF very tall (447 m) tower instrumented to measure fluxes of carbon, water, and energy between the land surface and the atmosphere [*Bakwin et al.*, 1998]. The site and the tower are located within the Chequamegon-Nicolet National Forest, and are both associated with the Chequamegon Ecosystem Atmosphere Study (ChEAS) [*Davis et al.*, 2003]. This area is located within the Northern Highlands physiographic province, which is a southern extension of the Canadian Shield. The bedrock is composed of Precambrian metamorphic and igneous rock, overlain by 8 to 90 m of glacial and glaciofluvial material. Topography of the area is slightly rolling, with an approximate variation in elevation of 3 m across most of the study site. Outwash, pitted outwash, and moraines are the dominant geomorphic features. The growing season is short and the winters are long and cold where mean July and January temperatures are 19°C and −12°C respectively [*Fassnacht and Gower*, 1997].

[7] The study site is a 120 m 120 m area that captures the transition between a forested upland and forest wetland (Figure 1). The forest is in secondary succession, regenerating from a timber harvest approximately 25 years ago. The upland is dominated by quaking aspen (*Populus tremuloides* Michx) with balsam fir (*Abies balsamea* (L.) Mill) also present in the overstory. Speckled alder (*Alnus incana* (DuRoi) Spreng) and white cedar (*Thuja occidentalis* L.) dominate the wetland. Aspen, alder, and cedar were identified as the dominant species for sap flux sampling (Table 1).

2.2. Data Collection

[8] Cyclic sampling was employed to establish plots for sap flux instrumentation [*Burrows et al.*, 2002]. We used a 3/7 cyclic sampling design (Figure 1), where three plots in seven are sampled, and this cycle is repeated. By using such an approach we were able to maximize the spatial information from our site while simultaneously minimizing the number of samples required to generate robust semivariograms. A total of 144 circular plots with a 5 m diameter were established, and the species and diameter at breast height of each tree in every plot was recorded. At least one tree per plot was selected for sap flux sampling. Trees were selected based on species with priority given to aspen, alder, and cedar, respectively. Where more than one member of a species was present the largest tree based upon diameter at breast height (DBH) was chosen. For each tree in each plot we recorded DBH, distance from the tree to the plot center, and the tree's direction from plot center. In plots with multiple species present, trees from each species were sampled with sap flux sensors where resources allowed. A total of 173 trees were instrumented in the site (Table 1). Trees were instrumented for sap flux measurements from 28 July to 6 August 2004 using Granier-type sensors [*Granier*, 1987], and data from 1, 3–5 August were used for analyses.

[9] Sapwood area (A_S) for each tree was calculated from DBH using species-specific allometric relationships established from a study within 10 km of the site [*Ewers et al.*, 2002]. Ewers' study reports a positive correlation between DBH and sapwood depth for all species except cedar, which exhibits a constant sapwood depth. In addition cedar was the only species to display circumferential differences in J_S, with slightly higher fluxes observed on the south side of stems. A radial decline in J_S was observed between 0–20 mm and 20–40 mm sapwood depth for aspen, and this

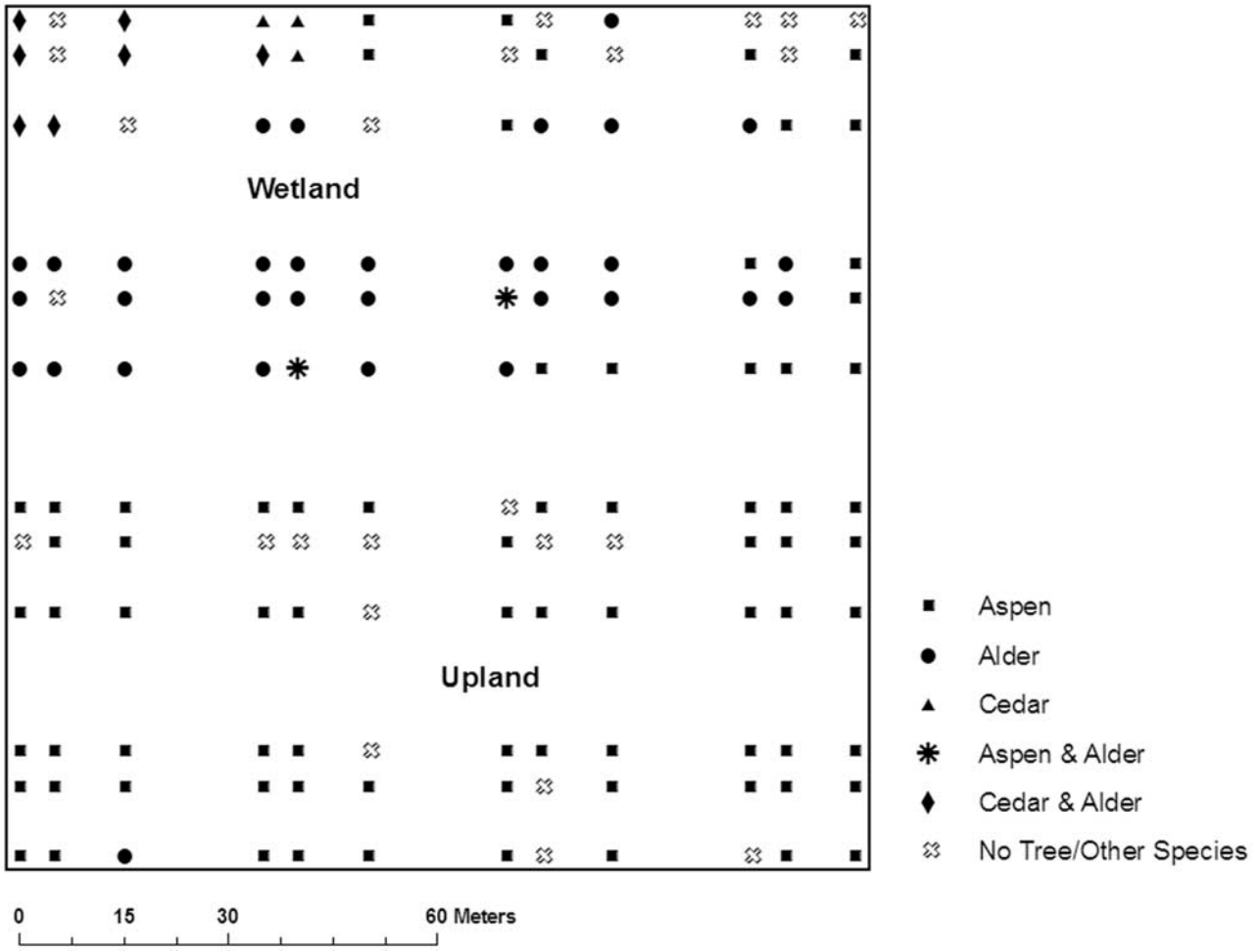

Figure 1. Map of the study site showing cyclic sampling design and species sampled for each plot.

relationship was independent of DBH and height. No trends are reported for Alder, however the relationship between DBH and sapwood depth differs from all other species that were sampled because there was no heartwood formation. From the results Ewers and colleagues were able to derive relationships between DBH and A_S capable of accurately scaling point measurements of J_S to E_C. We calculated observed transpiration per tree (E_{C-OBS}) with estimates of A_S based on the findings of *Ewers et al.* [2002] using the following equation:

$$E_{C-OBS} = J_S * A_S \quad (1)$$

where J_S is transpiration per unit xylem area (g m^{-2} sec^{-1}) measured within the active sapwood zone, and A_S is sapwood area (m^2). Note that E_{C-OBS} is transpiration for an individual tree, and not transpiration per unit ground area (E_{CG}) which is often reported. Scaling J_S to E_{CG} is accomplished by substituting the ratio of sapwood area to ground area for a plot (A_S: A_G) for A_S in equation (1) [*Oren et al.*, 1998]. To examine E_{CG} would be useful for determining whether net transpirative fluxes per unit ground area vary spatially near stand boundaries. However, it would be difficult to assess whether such variation was attributable to physiological differences between individual plants or rather to stem size and/or densities across a stand. As such we chose to examine transpiration per tree in order to highlight differences in transpiration attributable to physiological variation between individuals. Looking at individuals is crucial for identifying the mechanisms underlying any spatial autocorrelation.

[10] Temperature and relative humidity measurements (Vaisala HMP 45C, Vaisala Oyj, Helsinki, Finland) were made at two thirds canopy height, ~7 m. Sap flux and environmental measurements were recorded every 30 s (CR10X, Campbell Scientific, Logan, UT, USA) and aggregated to 30 m values. Volumetric surface soil moisture (0–6 cm) estimates for each plot were obtained on July 28th, 30th, and August 5th by averaging three measurements

Table 1. Number of Sampled (n), and Mean, Total, and Percent Sapwood Area, and Mean Daily Sap Flux per Unit Sapwood Area by Species for Alder, Aspen, and Cedar

Species	n*	Mean A_S, cm^2	Total A_S, cm^2	Mean J_S, g cm^{-2} day^{-1}
Alder	41	22.0 (1.5)	880	117.0 (8.8)
Aspen	79	36.8 (1.2)	2763	122.2 (5.7)
Cedar	9	123.0 (13.8)	1230	101.7 (11.0)

Values in parentheses are 1 standard error of the mean.
*n = Total number of individuals instrumented for sap flux sampling.

taken at random locations within each plot (Theta Probe, Delta-T, Cambridge, UK). Additional measurements including wind speed, photosynthetically active radiation (Q_0), and precipitation were obtained from the nearby Lost Creek eddy flux tower [*Cook et al.*, 2004].

2.3. Model Description

[11] The Terrestrial Regional Ecosystem Exchange Simulator (TREES) [*Ewers et al.*, 2007a, 2008; *Mackay et al.*, 2003a; *Samanta et al.*, 2007] was used to simulate transpiration per tree (E_{C-SIM}). Gaps in E_{C-OBS} because of isolated power and sensor failures necessitated simulating E_C so that a data set robust enough to conduct geostatistical analyses at finer temporal scales (i.e., binned by time or hourly D) could be achieved. Total above canopy radiation was partitioned into sun and shade canopy elements with beam, scattered and diffuse radiation components [*Spitters et al.*, 1986], using light extinction methods described by *Campbell and Norman* [1998]. Beam and diffuse radiation within the canopy were further partitioned into photosynthetically active radiation (Q_0) and near infrared radiation for each canopy element so that Q_0 could be used in simulating stomatal conductance. Simulated transpiration was calculating in each element with the Penman-Monteith [*Monteith*, 1965] combination equation to calculate E_{C-SIM}. The canopy is treated as two parallel "big leaves" representing the sun and shade elements, with separate element level stomatal conductances and E_C values calculated in each element. E_C values for each element were summed to obtain whole canopy transpiration per tree.

[12] Water flow through woody plants is driven by an increasingly negative water potential gradient between the soil and atmosphere at the leaf surface. Water stress at high rates of transpiration in woody plants is typically attributed to hydraulic stress induced by high atmospheric D [*Sperry et al.*, 1998; *Tyree and Sperry*, 1989]. Stomata close to prevent hydraulic failure at high D in response to increased leaf water potential that is caused by high transpiration rates although the signal is still unknown [*Franks*, 2004; *Mott and Parkhurst*, 1991]. Models exist that describe (G_S) as a function of environmental factors [*Jarvis*, 1976], or as a function of photosynthetic carbon uptake [*Ball et al.*, 1987]. G_S can also be defined in terms of Darcy's Law [*Whitehead and Jarvis*, 1981; *Whitehead et al.*, 1984]:

$$G_s = K_s \frac{A_s}{A_L} \frac{1}{D} (\psi_s - \psi_L - h\rho_w g) \tag{2}$$

where G_S is average canopy stomatal conductance, K_S is whole tree hydraulic conductance, A_S is sapwood area, A_L is leaf area, ψ_S is soil water potential, ψ_L is leaf water potential, h is water column height, ρ_w is the water density, and g is acceleration due to gravity. Empirical forms of equation (2) are commonly used in conjunction with the Penman-Monteith [*Monteith*, 1965] equation to estimate transpiration [*Bosveld and Bouten*, 2001; *Ewers et al.*, 2008; *Mackay et al.*, 2003a, 2003b; *Scanlon and Albertson*, 2003; *Van Wijk et al.*, 2000]. In TREES each canopy element conductance is treated as a function of turbulent transport defined by combining boundary layer conductance and vapor conductance of the canopy surface in series [*Campbell and Norman*, 1998], using a Jarvis equation [*Jarvis*, 1976] to model G_S. The Jarvis equation uses a series of multiplicative functions to constrain a theoretical maximum stomatal conductance (G_{smax}), and has the following form in TREES:

$$G_S = G_{Smax} * f_1(D) * f_2(Q_0) \tag{3}$$

$$f_1(D) = 1 - \delta D \tag{4}$$

$$f(Q_0) = \frac{Q_0}{Q_0 + \alpha} \tag{5}$$

where Q_0 is photosynthetically active radiation (μmol m^{-2} sec^{-1}). The parameters G_{smax}, δ, and α are theoretical maximum stomatal conductance, sensitivity of stomata to D, and absolute sensitivity to Q_0 respectively. The E_{C-SIM} values were simulated using a mean species leaf area (A_L) as reported by *Ewers et al.* [2002] for these stand types and described by *Oren et al.* [1999].

[13] A Monte Carlo sampling approach was used to generate parameter values from uninformed distributions. A comparison between E_{C-SIM} and E_{C-OBS} was assessed using a linear least squares analysis and evaluated using the slope of the best fit line and the index of agreement (IOA) [*Willmott*, 1982]. For our analyses we first sorted the simulation results by slope, and then simulations within the top 1% according to slope were sorted by IOA to find the best fit model.

$$IOA = 1 - \left(\frac{(E_{C-OBS} - E_{C-SIM})^2}{(|E_{C-SIM} - \bar{E}_{C-OBS}| + |E_{C-OBS} - \bar{E}_{C-OBS}|)^2} \right) \tag{6}$$

2.4. Data

[14] Individual trees identified as outliers [*Adelman et al.*, 2008] were removed from the data set using the following logic. For each species diurnal values of E_{C-OBS} for each tree were plotted to identify erratic behavior, and/or extreme values that indicated potential sensor issues, or physiological problems (i.e., defoliation or mortality). In addition, the slope and IOA for the corresponding models were examined. Trees were excluded when both slope < 0.80 and IOA < 0.80. These thresholds were chosen because trees with known sensor issues resulting in erroneous data values typically exhibited slope and IOA < 0.80. In addition, one aspen tree on the edge of the site was a remnant from before the site was clear-cut. This individual had a DBH of 31.9 cm, which was large in comparison to the mean DBH of 9.5 cm for all other aspen sampled for sap flux. While sap flux per unit sapwood area for this individual was within the range of values for the site, whole tree sap flux was well above the site average and had a profound affect on the structure of the semivariograms because differences are squared (see below). This individual was ultimately excluded from the analysis on the grounds that it was not a true member of the regenerating stand.

[15] Half-hourly data values of J_S, and E_{C-SIM} were sorted according to D, and then aggregated into bins of

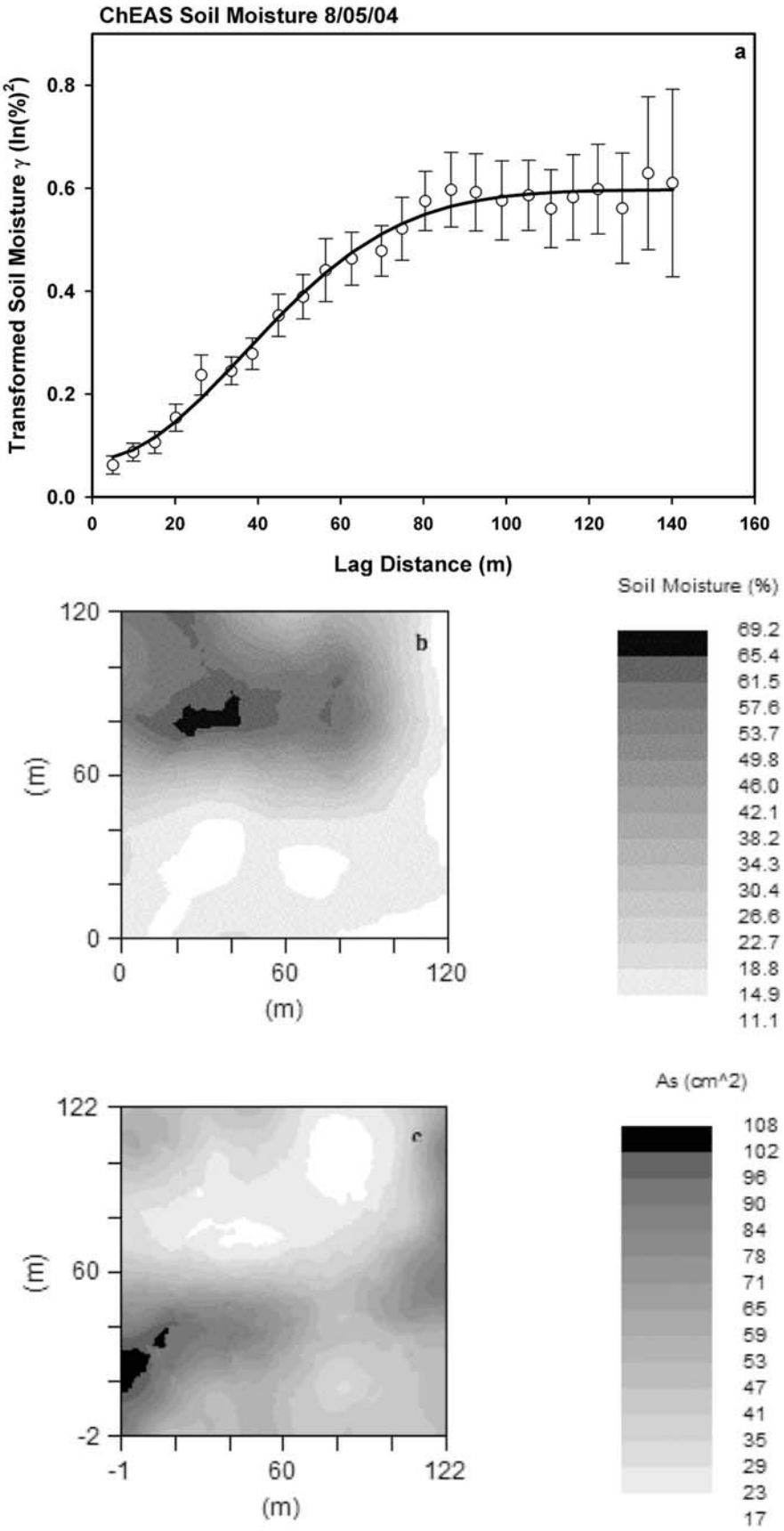

Figure 2. Semivariogram of soil moisture ($r^2 = 0.99$) for the study site (a) and corresponding kriged map (b), and a kriged map of A_S (c) for the study site. Note that kriged maps in this study are intended to aid interpretation of spatial patterns described by semivariograms, and not as predictions.

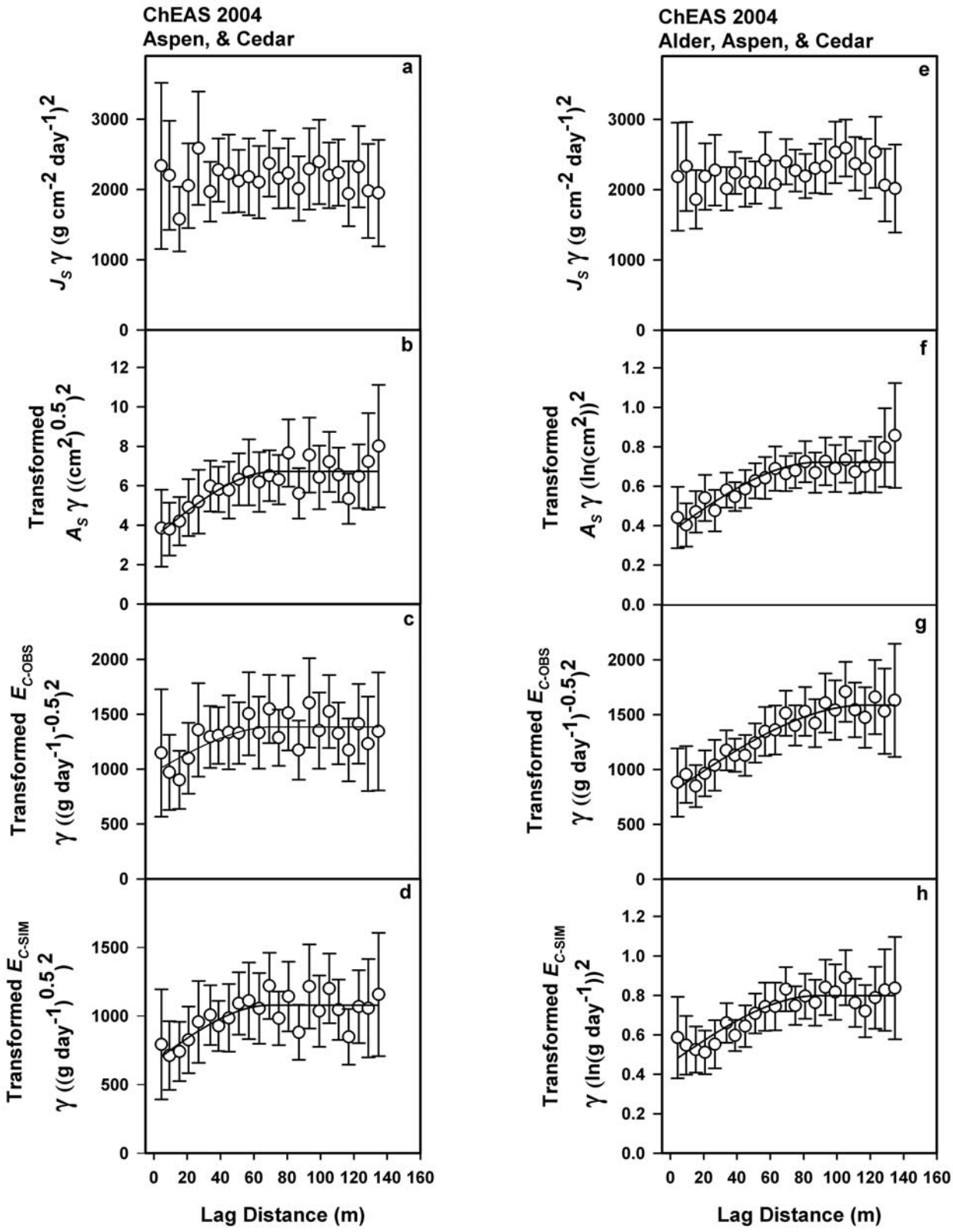

Figure 3. Semivariograms for 2-species sap flux (J_S) (a), 2-species sapwood area (A_S) (b), 2-species observed transpiration ($E_{C-\mathrm{OBS}}$) (c), 2-species simulated transpiration ($E_{C-\mathrm{SIM}}$) (d), 3-species sap flux (J_S) (e), 3-species sapwood area (A_S) (f), 3-species observed transpiration ($E_{C-\mathrm{OBS}}$) (g), and 3-species simulated transpiration ($E_{C-\mathrm{SIM}}$) (h). All semivariograms shown are plotted with 95% confidence intervals (equation (8)).

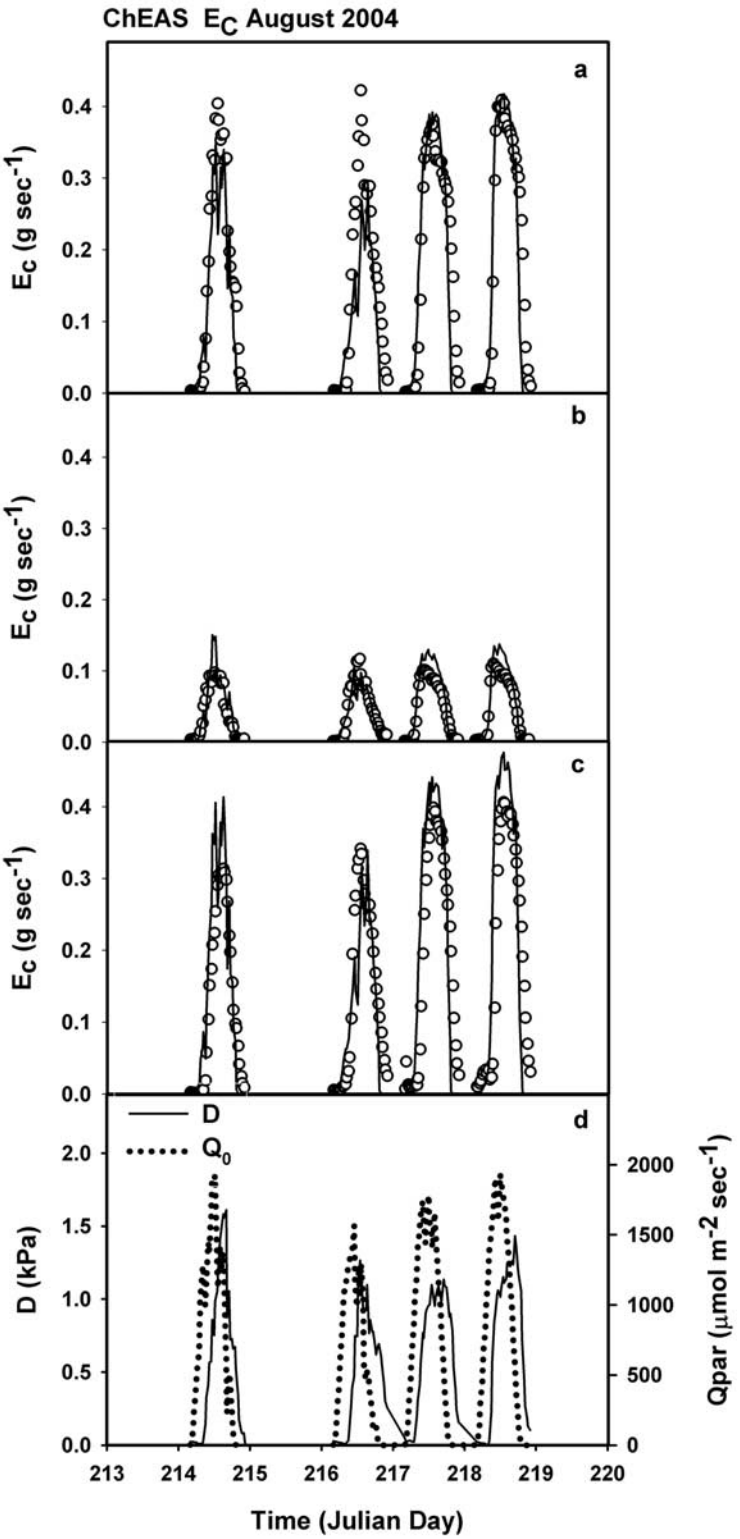

Figure 4. Time series of observed transpiration ($E_{C-\mathrm{OBS}}$) and modeled transpiration ($E_{C-\mathrm{SIM}}$) for alder (a), aspen (b), and cedar (c), and (d) vapor pressure deficit (D) and photosynthetically active radiation (Q_0) for 1, 3–5 August 2004.

0.2 kPa in order to examine trends in spatial variability with this environmental driver. We found this approach to be the more effective than binning by time or Q_0 for elucidating temporal trends in spatial patterns. This is likely due to the known relationship between D and G_S described by *Oren et al.* [1999] and general lack of one-to-one relationship between D and time.

Table 2. Mean Slope and IOA for EC-SIM by Species

Species	Mean Slope	Mean IOA
Alder	0.99 (0.006)	0.88 (0.03)
Aspen	0.98 (0.011)	0.90 (0.01)
Cedar	0.97 (0.007)	0.89 (0.01)

Values in parentheses are 1 standard error of the mean. Sample sizes are given in Table 1.

2.5. Statistical Analysis

[16] We employed geostatistics to examine our fluxes spatially, using the semivariogram. Semivariance was calculated using the following equation:

$$\gamma(h) = \frac{1}{2N(h)} \sum_{(i,j)|h_i=h} \left(v_i - v_j\right)^2 \quad (7)$$

where $\gamma(h)$ is the semivariance between two points separated by a lag distance (h), (v) is the difference in values between pairs of points (i, j) separated by h, and $N(h)$ = the total number of point pairs separated by h. A semivariogram is created by plotting h on the abscissa, and $\gamma(h)$ on the ordinate.

[17] Geostatistical analyses were performed with GS+ (version 7, Gamma Design Software, Plainwell, MI, USA). Common semivariogram models assume normally distributed data [*Cressie*, 1993; *Diggle et al.*, 1998], and so for each variable analyzed using geostatistics we applied one of two available transformations, log or square root, if they resulted in a distribution closer to normal than the untransformed data. Skewness of the distribution was used to gauge normalcy and determine whether transformation yielded an improvement. Spherical models were fit manually to minimize the residual sum of squares, and maximize R^2. Differences in the absolute semivariance (i.e., the sill) result from different transformations. Relativized semivariograms were created by relativizing equation (8) to a sill of 1 [*Isaaks and Srivasta*, 1989] for each semivariogram model. The following equation was used to calculate 95 percent confidence intervals for the semivariograms:

$$Cl_{95} = 1.96\frac{\sqrt{2\gamma}}{\sqrt{N}} \quad (8)$$

where γ is the semivariance of a lag class of points with separation distance h, and N is the number of point pairs within the lag class. We analyzed drift to detect spatial trends in mean and variance that would violate the assumption of second order stationarity associated with geostatistics [*Legendre and Legendre*, 1998]. Where trends were identified appropriate de-trending measures were taken.

[18] Semivariograms are useful for quantifying spatial autocorrelation. However, in order to relate autocorrelation to geographic locations additional tools must be employed. Interpolated maps are typically used for this purpose, and kriging is a method exclusive to geostatistics that is designed to minimize error variance. Kriging produces estimates based on a weighted linear combination of the covariance of nearby sample points, accounting for statistical rather than geographic distance between pairs of points. We use the point kriging method of interpolation to create maps displaying spatial patterns in transpiration. Our maps are intended to be visual aids, and not predictions. All transformed data were back transformed for interpolation.

[19] Regression analysis was performed in Sigmaplot (version 9.01 Systat Software, CA, USA).

3. Results

[20] Soil moisture across the site exhibited strong spatial autocorrelation (Figures 2 and 3). The soil moisture semivariogram had a range of 90 m ($r^2 = 0.99$) and the structural variance represented 88 percent of the total variance. The semivariograms of mean daily J_S revealed no spatial autocorrelation between values across the site (Figure 3). Examination of the semivariograms for A_S, mean daily E_{C-OBS}, and mean daily E_{C-SIM} revealed drift, which violated the assumption of second-order stationarity. For data used in these semivariograms the variance increased with increasing separation distance indicating a bimodal distribution. This trend was the result of the differences in mean values of A_S between alder, and aspen and cedar, and so we conducted a parallel set of analyses using a detrended data set consisting of only aspen and cedar. Hereafter all analyses conducted using alder, aspen, and cedar are denoted as 3-species, and those using only aspen and cedar are denoted as 2-species.

[21] As shown by both 2-species and 3-species semivariograms of A_S (Figure 3), there was spatial autocorrelation among the samples. Ranges of 73 m ($r^2 = 0.73$) and 89 m ($r^2 = 0.85$), and proportions of structural variance of 0.50 and 0.49 were observed for 2-species A_S and 3-species A_S, respectively. Similar results were obtained for both 2-species and 3-species mean daily E_{C-OBS}, and 2-species and 3-species mean daily E_{C-SIM}. For 2-species and 3-species mean daily E_{C-OBS}, respectively, ranges of 72 m ($r^2 = 0.47$) and 118 m ($r^2 = 0.93$) and proportions of structural variance of 0.30 and 0.50 were observed. Semivariograms of 2-species and 3-species mean daily E_{C-SIM} respectively exhibited ranges of 70 m ($r^2 = 0.59$) and 89 m ($r^2 = 0.81$), and proportions of structural variance of 0.37 and 0.43.

[22] Figure 4 shows average E_{C-OBS} and E_{C-SIM} for each species along with D and Q_0 for four days in August 2004. E_{C-SIM} matched E_{C-OBS} values reasonably well (Table 2). Mean slope and IOA values for alder, aspen, and cedar were 0.99 and 0.88, 0.98 and 0.90, and 0.97 and 0.89 respectively. Diurnal patterns of E_{C-OBS} and E_{C-SIM} responded to D as expected. A 2 h lag in the response of D to changes in Q_0 was observed as well (Figure 4).

[23] Analyses of binned mean hourly E_{C-SIM} exhibited little spatial autocorrelation, and no discernable changes in spatial autocorrelation with time were observed (data not shown). Analyses of E_{C-SIM} binned by Q_0 yielded similar results (data not shown). Subsequent analyses of E_{C-SIM} binned by D revealed differences in spatial autocorrelation across bins. Figure 5 shows the actual semivariograms, relativized semivariograms, and corresponding kriged maps for bins of 2-species E_{C-SIM} where mean D = 0.30 kPa, D = 0.92 kPa, and D = 1.51 kPa with ranges of 87 m ($r^2 = 0.57$), 69 m ($r^2 = 0.53$), and 48 m ($r^2 = 0.44$) respectively. Figure 6 shows the actual semivariograms, relativized semivariograms, and corresponding kriged maps for bins of 3-species E_{C-SIM} where mean D = 0.30 kPa, D = 0.92 kPa, and D =

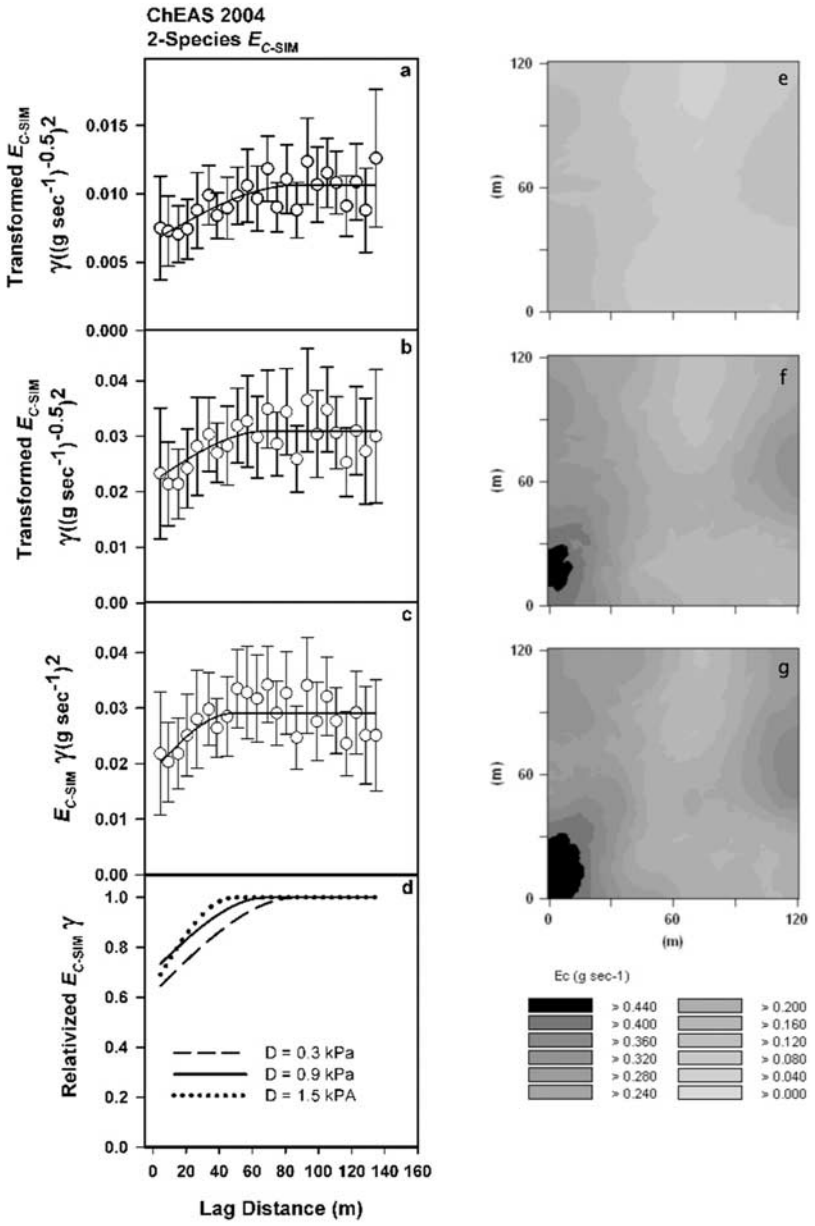

Figure 5. Semivariograms for 2-species $E_{C\text{-SIM}}$ binned by (a) D = 0.3 (r^2 = 0.57), (b) 0.9 (r^2 = 0.53), and (c) 1.5 (r^2 = 0.50), and (d) relativized by sill semivariograms for all three bins. Corresponding kriged maps of 2-species $E_{C\text{-SIM}}$ where D = 0.3 kPa (e), D = 0.9 kPa (f), D = 1.5 kPa (g). Actual semivariograms shown are plotted with 95% confidence intervals (equation (8)). Note that kriged maps in this study are intended to aid interpretation of spatial patterns described by semivariograms, and not as predictions.

1.51 kPa with ranges of 101 m (r^2 = 0.84), 100 m (r^2 = 0.88), and 82 m (r^2 = 0.81), respectively. The range of E_{C-SIM} spatial autocorrelation was negatively correlated with D for all data (Figure 7). Slopes of −25.7 (r^2 = 0.89; $p < 0.001$), and −24.1 (r^2 = 0.78; $p < 0.001$) were observed for 2-species and 3-species E_{C-SIM} respectively.

4. Discussion

[24] Our results show that spatial autocorrelation exists in forest canopy transpiration across an aspen-dominated upland-to-wetland transition. We rejected our first hypothesis due to the absence of spatial autocorrelation in the semivariograms for 2-species and 3-species J_S (Figure 3). Conversely, given the spatial autocorrelation exhibited in semivariograms for 2-species and 3-species E_{C-OBS} and E_{C-SIM} (Figure 3) meant that we failed to reject our second and third hypotheses. Our results indicate that spatial autocorrelation in E_C (E_{C-OBS} and E_{C-SIM}) is an effect of scaling J_S by A_S. Our model was able to effectively simulate transpiration for each species we measured, and replicate the patterns of spatial autocorrelation present in the data. Semi-

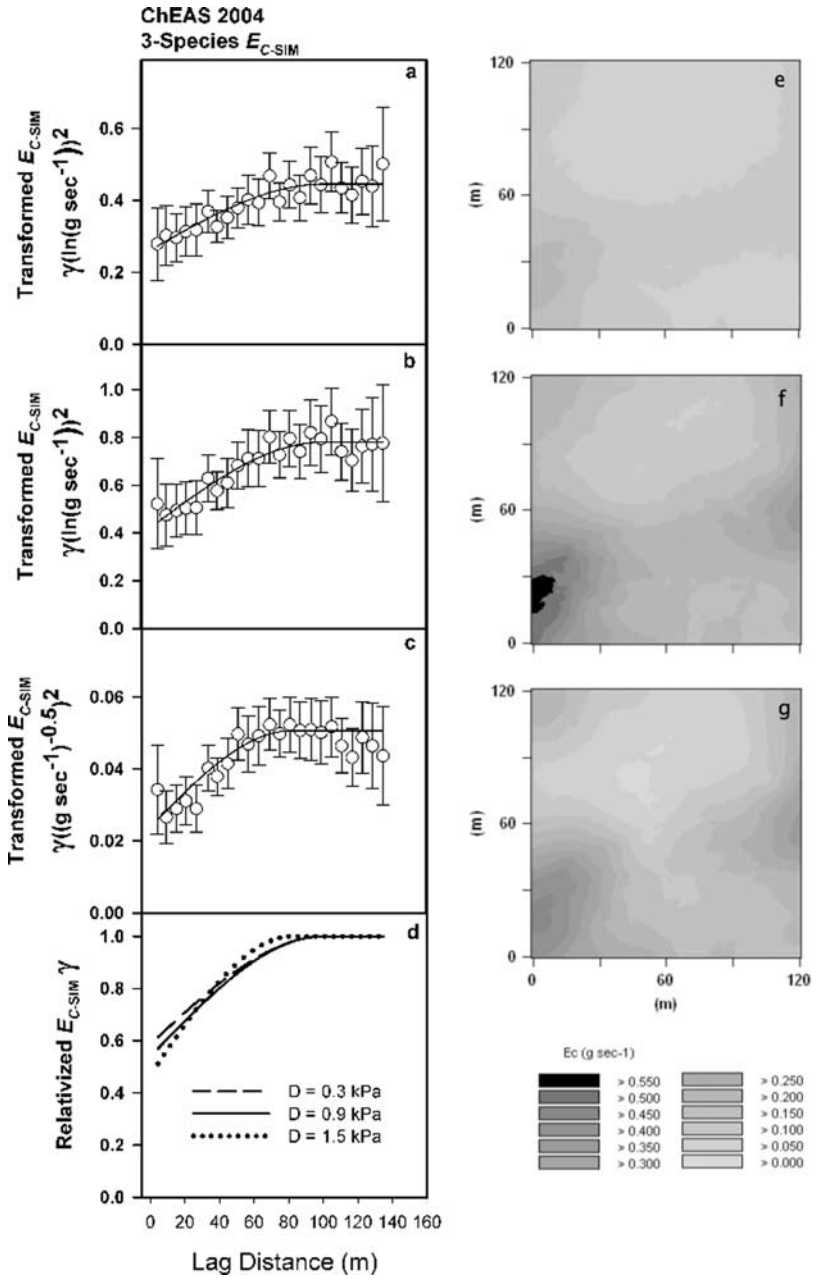

Figure 6. Actual semivariograms for 3-species $E_{C\text{-SIM}}$ binned by (a) $D = 0.3$ ($r^2 = 0.84$), (b) 0.9 ($r^2 = 0.88$), and (c) 1.5 ($r^2 = 0.88$) and (d) relativized by sill semivariograms for all three bins. Corresponding kriged maps of 3-species $E_{C\text{-SIM}}$ where $D = 0.3$ (e), D = 0.9 (f), D = 1.5 (g). Actual variograms shown are plotted with 95% confidence intervals (equation (8)). Note that kriged maps in this study are intended to aid interpretation of spatial patterns described by semivariograms, and not as predictions.

variograms of 2-species and 3-species E_{C-OBS} and E_{C-SIM} binned by D indicated a dynamic pattern of spatial autocorrelation, and therefore we failed to reject hypothesis 4.b. (Hypothesis 4.a was precluded from analysis and therefore rejected because the first hypothesis was rejected.) Interestingly, we found the range of spatial autocorrelation to be negatively correlated with D, indicating that A_S is not solely responsible for spatial variation in E_C so that scaling in space requires knowledge of responses of key attributes, namely G_S, to variation in temporal drivers such as D.

4.1. Spatial Patterns of J_s

[25] We expected J_S fluxes to vary, both within and between species along the observed gradient in soil moisture across the site. Possibly, this failed to occur because the upland plots, although much drier then the wetland plots, had sufficient moisture so that soil moisture was not limiting transpiration. It should be noted that our soil moisture measurements characterized the upper 6 cm of the soil, which may not be indicative of moisture availability in the entire root zone and probably underestimated it

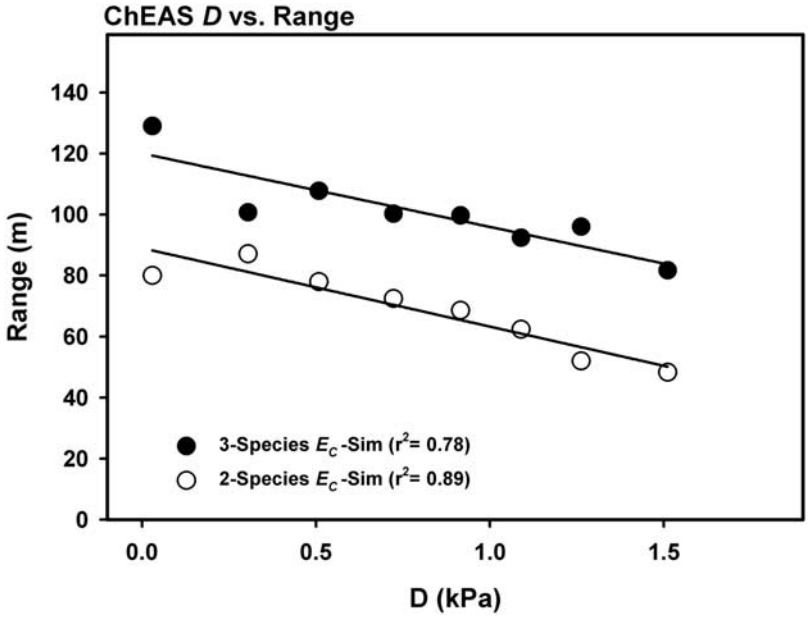

Figure 7. Plot of D versus Range (equation (12)) of spatial autocorrelation for 2- and 3-species $E_{C-\mathrm{SIM}}$ with regression lines.

[*Wilson et al.*, 2003]. However, soil moisture rarely limits transpiration in these forests [*Desai et al.*, 2005; *Ewers et al.*, 2002, 2007a; *Mackay et al.*, 2002, 2007].

[26] Characteristics of the species observed in this study likely contributed to the lack of structure in the spatial variation of J_S as well. In the wetland, alder and cedar were not water limited as the water table was typically within 1m of the surface as evidenced by piezometer observations across a wide range of environmental conditions in subsequent field seasons. The relative lack of aspen in the wetland (Figure 1) was consistent with its comparative intolerance of excess water [*Landhausser et al.*, 2003]. On the other hand, minimal variation in J_S among the upland aspen is consistent with reports that the species is relatively drought tolerant and has exhibited relatively little sensitivity to moisture limitation even in xeric environments [*Hogg et al.*, 2000; *Pataki et al.*, 2000].

4.2. Spatial Patterns of E_c

[27] Following equation (4) and the semivariograms for J_S, A_S, E_{C-OBS}, and E_{C-SIM} for both 2-species and 3-species (Figure 3) it is clear that spatial patterns of A_S explained the spatial patterns of E_{C-OBS} and E_{C-SIM}. A positive correlation between A_S and E_C may also be inferred from a visual comparison of their respective kriged maps (Figure 2). Our results suggest that traditional estimates of stand transpiration derived using A_S from trees sampled within a representative plot to scale mean J_S to E_C [*Oren et al.*, 1998; *Ewers et al.*, 1999, 2002, 2008; *Hatton et al.*, 1995] should consider the location of the plot. In order for this approach to yield an accurate estimate of stand E_C the representative plot would have to be located in an area representative of mean spatial whole-tree E_C, i.e., near a stand boundary in our case. Situating a plot near the center of a stand may preclude trees from the lower end of mean E_C distribution, particularly where plot sizes are small, and/or the stand is substantially larger than the typical plot size (~30 m). Although the assumption of spatially well-mixed transpiration per tree does not hold for this site, this scaling method still applies because the spatial pattern of transpiration can be attributed to spatial patterns of A_S, which can be inexpensively measured spatially through its allometric relationship with DBH. In water-limited ecosystems where spatial patterns of E_C may be driven by spatially variable J_S, up-scaling may be more complicated, requiring spatially explicit sampling of J_S.

[28] Our results emphasize the importance of considering ecological boundaries. A biological perspective may be appropriate for exploring the spatial pattern of transpiration at this site in the sense that it is the physical size of individuals that dictates E_C. In order to understand this spatial pattern it may be necessary to consider environmental constraints exerted by biophysical characteristics throughout the site such as competition between species, and in the case of aspen the possible growth limiting effects of excessive soil moisture in the wetland. Kriged maps in Figure 2 suggest that A_S is negatively correlated with soil moisture at our site. Differences in decomposition rates and subsequent nutrient turnover, or simply anoxia alone could cause such differences in growth rates which lead to differences in A_S between the upland and wetland. Accounting for boundary gradients characterized by spatial patterns of dominant species may improve regional E_C estimates as well, especially as forests such as this one are increasingly fragmented by natural and anthropogenic disturbances [*Vitousek et al.*, 1997].

4.3. Intraspecific Versus Interspecific Species Effects

[29] We found that comparing E_C between species violated the assumption of stationarity associated with geostatistical analyses. To overcome this we chose to examine only species with similar E_C values. The presence of a trend in the 3-species data set exposes several issues that need to be considered in the context of studies examining spatial

transpiration. Understanding changes in processes such as transpiration per tree across ecosystem boundaries is important for scaling up and understanding ecosystem processes. However, species differences that are likely to be of interest may exacerbate the magnitude of variation across such transitions. This is particularly important to consider in the context of the techniques employed here where species differences created additional spatial autocorrelation on a per tree basis. This suggests that a more suitable approach may be to preclude trends by initially examining one species at a time. This is reflected in the focus on aspen in the interpretation of our results. Aspen comprises nearly 90 percent of the 2-species data set, and is a more important species in the region from a hydrological perspective in terms of its abundance and high rates of transpiration [*Ewers et al.*, 2002, 2007a; *Mackay et al.*, 2002]. The spatial extent and sample size for each species prohibited geostatistical analysis for individual species. We retained results from analyses of the 3-species data as support for the 2-species results and to illustrate the effects of sample size on our semivariance confidence intervals.

4.4. Drivers of Spatial E_c

[30] On average, simulations of E_C fit the observed data reasonably well. Noticeable deviations occurred during midday periods of high D. Here some spikes in E_{C-OBS} were not reproduced by E_{C-SIM}. It is possible that these spikes were not in response to D or to Q_0, but rather a result of some other physiological or physical process such as a delayed stomatal response to D, or canopy self shading [*Beadle et al.*, 1985; *Ewers et al.*, 2007b; *Zweifel et al.*, 2002]. Semivariograms of E_{C-SIM} were smoother than those for E_{C-OBS} for both 2-species and 3-species. E_{C-OBS} data contains gaps, while E_{C-SIM} is continuous throughout the time period and this likely contributes to the smoothing effect exhibited in the analyses. Additionally, the model is driven by both D and Q_0, and as such estimates exhibit a strong response to these variables. Our model performs well at times when Q_0 typically limits E_C during periods of low D in early morning and late afternoon so we can exclude it as an explanation for discrepancies between E_{C-SIM} and E_{C-OBS}. Our results indicate that soil moisture is not likely to offer an explanation. Temperature can be eliminated as an explanation as well because our data was collected on warm summer days with midday temperatures in excess of 20°C on all days used for analyses. Currently no other variables that affect E_C and that would allow it to respond to other drivers are incorporated into the model. Additional variables may be required to improve model accuracy. Temporal variation in the proportion of sunlit versus shaded leaves and Q_0 due to inter and intracanopy interactions is a possible inclusion that may improve the model.

4.5. Dependence of Spatial Patterns of E_c on D

[31] The general response of E_C to D observed in our results agreed with common findings from the literature [*Oren et al.*, 2001]. However, it is unlikely that changes in E_C spatial heterogeneity were caused by differences in D among plots. Aspen canopies are typically well coupled with the atmosphere due to their rotating petiole [*Hogg and Hurdle*, 1997], and atmospheric D should be relatively homogenous above and within the canopy at the scale of this study [*Jarvis and McNaughton*, 1986] which has been verified in these forests by comparing D between a forested wetland, an aspen stand and above canopy [*Ewers et al.*, 2008]. A plausible explanation is physiological differences manifested in G_S. There is tree-to-tree variation in J_S, but no autocorrelation could be detected with variogram analysis. However, individual tree responses to increasing rates of E_C require that K_S drops in response to lower water potentials. This reduces the effective sapwood area while having no effect on J_S. Physically this can be described in terms of the response of K_S to changes in ψ_L as E_C increases. Potential determinants of sensitivity to water loss rate may include soil textural effects on K_S, [*Hacke et al.*, 2000], nutrient impacts [*Ewers et al.*, 2008], competition for light effects on photosynthetic limitations to G_S, and topographic position [*Franks*, 2004; *Mott and Parkhurst*, 1991; *Sperry et al.*, 1998; *Tyree and Sperry*, 1989]. Future research is aimed at testing this hypothesis with more detailed measurements and TREES.

[32] Another possible cause for the changes in the range of E_C semivariograms are variations in shading within the canopy caused by competition for light between individuals which is probably manifest in the increased variability in E_{C-OBS} during high fluxes (Figure 4). Values of D typically follow a diurnal pattern that peaks after mid day and lower D values typically occur closer to sunrise and sunset when zenith angles are lowest. As such the proportion of sunlit and shaded leaves may exhibit temporal variation accordingly. Concurrently, spatial variation in the proportion of sunlit versus shade leaves as a result of competitive shading likely exists as well. This could be due to either tree height heterogeneity, and/or the presence of remnants from previous stands interspersed throughout the site. Although our model incorporates sunlit and shaded canopy elements, spatially accounting for temporal variation in the proportion of these elements could explain some of the variation of E_C range with D [*Boulain et al.*, 2007].

[33] In light of this result, variation in spatial patterns of E_C with D over time becomes very important in the context of scaling up to landscape and regional scales. Simply considering spatial patterns may not be sufficient to calculate accurately scaled estimates of E_C. A more sophisticated scaling approach that involves a temporal consideration of environmental drivers and subsequent effects on spatial patterns of E_C may be required. The ability of the model to capture such temporal variation in spatial patterns (Figures 5 and 6) suggests that we are close to accomplishing this.

4.6. Implications for Landscape Scale E_c

[34] Our results suggest that it is necessary to consider landscape heterogeneity in relation to E_C. It may no longer be sufficient to rely on general vegetation classification and a few key environmental variables to create adequate estimates of E_C or evapotranspiration (ET). By incorporating atmospheric and edaphic drivers in up-scaling efforts, and doing so in a spatial context, more accurate estimates will be achieved. Ecological gradients and stand boundaries are becoming more easily identifiable with increasingly available high resolution remote sensing data. General spatial patterns could be captured by including edaphically controlled drivers such as soil texture, moisture,

or nutrients. Spatially explicit estimates could be further refined by including atmospheric drivers such as D that effect spatial patterns temporally. Ideally, further investigation will elucidate links between E_C and these spatial drivers, with the ultimate goal of improving predictive understanding by discovering the mechanisms behind spatially varying transpiration.

5. Conclusions

[35] Using geostatistics we have shown that transpiration per tree varies spatially across an aspen dominated upland-to-wetland transition in northern Wisconsin. Spatial variation was not exhibited in transpiration per unit xylem area, but was observed in sapwood area. As such it appears that spatial patterns for individual species are the key to obtaining more accurate estimates of stand transpiration, and that future efforts to characterize such patterns may rely on simple species relationships with environmental drivers rather than geospatial techniques. This suggests that scaling to the stand level may be accomplished using traditional methods if the representative plot is located in an area that captures mean spatial E_C, despite the apparent invalidity of the assumption that transpiration is homogenous at the stand level. We have shown that a simple model is capable of replicating species specific spatial patterns observed in field data. Spatial patterns of whole-tree transpiration changed temporally with D, indicating that scaling efforts should consider spatial and temporal heterogeneity in relation to D. This demonstrates that models relying on soil moisture gradients as primary limiting factors of spatial transpiration are insufficient at this particular site, underscoring the importance of seeking alternative ecohydrological controls on water fluxes and not just soil water in forest ecosystems, which in many regions are not typically water-limited. On the contrary, we suggest that excessively high soil moisture near and within the wetland had a long-term effect of limiting tree growth and thus only in the long-term contributed to spatial autocorrelation in E_C.

[36] **Acknowledgments.** Funding for this study was from the National Science Foundation, Hydrologic Sciences Program (EAR-0405306 to D.S.M., EAR-0405381 to B.E.E., and EAR-0405318 to E.L.K.). In addition, M.L. was supported by the NSF IGERT program. The statements made in this manuscript reflect the views of the authors and do not necessary reflect the views of NSF. We would also like to thank personnel at Kemp Natural Resource Station in Woodruff, Wisconsin for logistical support.

References

Adelman, J. A., B. E. Ewers, and D. S. Mackay (2008), Using temporal patterns in vapor pressure deficit to explain spatial autocorrelation dynamics in tree transpiration, *Tree Physiol.*, *28*, 647–658.

Alsheimer, M., B. Kostner, E. Falge, and J. D. Tenhunen (1998), Temporal and spatial variation in transpiration of Norway spruce stands within a forested catchment of the Fichtelgebirge, Germany, *Ann. Sci. Forestieres*, *55*(1–2), 103–123.

Bakwin, P. S., P. P. Tans, D. F. Hurst, and C. L. Zhao (1998), Measurements of carbon dioxide on very tall towers: Results of the NOAA/CMDL program, *Tellus, Ser. B-Chem. Phys. Meteorol.*, *50*(5), 401–415.

Ball, J. T., I. E. Woodrow, and J. A. Berry (1987), A model predicting stomatal conductance and its contribution to the control of photosynthesis under different environmental conditions, in *Progress in Photosynthesis Research*, edited by J. Biggens, pp. 221–224, Martinus Nijhoff, Dordrecht.

Band, L. E. (1993), Effect of land-surface representation on forest water and carbon budgets, *J. Hydrol.*, *150*(2–4), 749–772.

Band, L. E., and I. D. Moore (1995), Scale-landscape attributes and geographical information-systems, *Hydrol. Processes*, *9*(3–4), 401–422.

Beadle, C. L., R. E. Neilson, H. Talbot, and P. G. Jarvis (1985), Stomatal conductance and photosynthesis in a mature scots pine forest. 1. Diurnal, seasonal and spatial variation in shoots, *J. Appl. Ecol.*, *22*(2), 557–571.

Bosveld, F. C., and W. Bouten (2001), Evaluation of transpiration models with observations over a Douglas-fir forest, *Agric. For. Meteorol.*, *108*(4), 247–264.

Boulain, N., G. Simioni, and J. Gignoux (2007), Changing scale in ecological modelling: A bottom up approach with an individual based vegetation model, *Ecol. Modell.*, *203*(3–4), 257–269.

Burrows, S. N., S. T. Gower, M. K. Clayton, D. S. Mackay, D. E. Ahl, J. M. Norman, and G. Diak (2002), Application of geostatistics to characterize leaf area index (LAI) from flux tower to landscape scales using a cyclic sampling design, *Ecosystems*, *5*(7), 667–679.

Campbell, G. S., and J. M. Norman (1998), *An Introduction to Environmental Biophysics*, 2nd ed., Springer-Verlag, New York.

Cermak, J., E. Cienciala, J. Kucera, A. Lindroth, and E. Bednarova (1995), Individual variation of sap-flow rate in large pine and spruce trees and stand transpiration - A pilot-study at the Central Nopex site, *J. Hydrol.*, *168*(1–4), 17–27.

Cook, B. D., et al. (2004), Carbon exchange and venting anomalies in an upland deciduous forest in northern Wisconsin, USA, *Agric. For. Meteorol.*, *126*(3–4), 271–295.

Cressie, N. (1993), *Statistics for Spatial Data*, Revised ed., Wiley, New York.

Davis, K. J., P. S. Bakwin, C. X. Yi, B. W. Berger, C. L. Zhao, R. M. Teclaw, and J. G. Isebrands (2003), The annual cycles of CO2 and H2O exchange over a northern mixed forest as observed from a very tall tower, *Global Change Biol.*, *9*(9), 1278–1293.

Desai, A. R., P. V. Bolstad, B. D. Cook, K. J. Davis, and E. V. Carey (2005), Comparing net ecosystem exchange of carbon dioxide between an old-growth and mature forest in the upper Midwest, USA, *Agric. For. Meteorol.*, *128*(1–2), 33–55.

Diggle, P. J., J. A. Tawn, and R. A. Moyeed (1998), Model-based geostatistics, *J. R. Stat. Soc., Ser. C-Appl. Stat.*, *47*, 299–326.

Ewers, B. E., R. Oren, T. J. Albaugh, and P. M. Dougherty (1999), Carry-over effects of water and nutrient supply on water use of Pinus Taeda, *Ecol. Appl.*, *9*(2), 513–525.

Ewers, B. E., R. Oren, and J. S. Sperry (2000), Influence of nutrient versus water supply on hydraulic architecture and water balance in Pinus taeda, *Plant Cell Environ.*, *23*(10), 1055–1066.

Ewers, B. E., D. S. Mackay, S. T. Gower, D. E. Ahl, S. N. Burrows, and S. S. Samanta (2002), Tree species effects on stand transpiration in northern Wisconsin, *Water Resour. Res.*, *38*(7), 1103, doi:10.1029/2001WR000830.

Ewers, B. E., D. S. Mackay, and S. Samanta (2007a), Interannual consistency in canopy stomatal conductance control of leaf water potential across seven tree species, *Tree Physiol.*, *27*(1), 11–24.

Ewers, B. E., R. Oren, H. S. Kim, G. Bohrer, and C. T. Lai (2007b), Effects of hydraulic architecture and spatial variation in light on mean stomatal conductance of tree branches and crowns, *Plant Cell Environ.*, *30*(4), 483–496.

Ewers, B. E., D. S. Mackay, J. Tang, P. Bolstad, and S. Samanta (2008), Intercomparison of sugar maple stand transpiration responses to environmental conditions for the western great lakes region of the United States, *Agric. For. Meteorol.*

Famiglietti, J. S., and E. F. Wood (1994), Multiscale modeling of spatially-variable water and energy-balance processes, *Water Resour. Res.*, *30*(11), 3061–3078.

Fassnacht, K. S., and S. T. Gower (1997), Interrelationships among the edaphic and stand characteristics, leaf area index, and aboveground net primary production of upland forest ecosystems in north central Wisconsin, *Can. J. For. Res. -Revue Canadienne De Recherche Forestiere*, *27*(7), 1058–1067.

Foley, J. A., I. C. Prentice, N. Ramankutty, S. Levis, D. Pollard, S. Sitch, and A. Haxeltine (1996), An integrated biosphere model of land surface processes, terrestrial carbon balance, and vegetation dynamics, *Global Biogeochem. Cycles*, *10*(4), 603–628.

Foley, J. A., S. Levis, M. H. Costa, W. Cramer, and D. Pollard (2000), Incorporating dynamic vegetation cover within global climate models, *Ecol. Appl.*, *10*(6), 1620–1632.

Franks, P. J. (2004), Stomatal control and hydraulic conductance, with special reference to tall trees, *Tree Physiol.*, *24*(8), 865–878.

Gallardo, A., and F. Covelo (2005), Spatial pattern and scale of leaf N and P concentration in a Quercus robur population, *Plant Soil*, *273*(1–2), 269–277.

Gazal, R. M., R. L. Scott, D. C. Goodrich, and D. G. Williams (2006), Controls on transpiration in a semiarid riparian cottonwood forest, *Agric. For. Meteorol.*, *137*(1–2), 56–67.

Gedney, N., P. M. Cox, R. A. Betts, O. Boucher, C. Huntingford, and P. A. Stott (2006), Detection of a direct carbon dioxide effect in continental river runoff records, *Nature*, *439*(7078), 835–838.

Granier, A. (1987), Evaluation of transpiration in a Douglas-fir stand by means of sap flow measurements, *Tree Physiol.*, *3*(4), 309–319.

Granier, A., P. Biron, and D. Lemoine (2000), Water balance, transpiration and canopy conductance in two beech stands, *Agric. For. Meteorol.*, *100*(4), 291–308.

Grayson, R. B., G. Bloschl, A. W. Western, and T. A. McMahon (2002), Advances in the use of observed spatial patterns of catchment hydrological response, *Adv. Water Resour.*, *25*(8–12), 1313–1334.

Hacke, U. G., J. S. Sperry, B. E. Ewers, D. S. Ellsworth, K. V. R. Schafer, and R. Oren (2000), Influence of soil porosity on water use in Pinus taeda, *Oecologia*, *124*(4), 495–505.

Hatton, T. J., S. J. Moore, and P. H. Reece (1995), Estimating stand transpiration in a Eucalyptus-populnea woodland with the heat pulse method - Measurement errors and sampling strategies, *Tree Physiol.*, *15*(4), 219–227.

Hogg, E. H., and P. A. Hurdle (1997), Sap flow in trembling aspen: Implications for stomatal responses to vapor pressure deficit, *Tree Physiol.*, *17*(8–9), 501–509.

Hogg, E. H., B. Saugier, J. Y. Pontailler, T. A. Black, W. Chen, P. A. Hurdle, and A. Wu (2000), Responses of trembling aspen and hazelnut to vapor pressure deficit in a boreal deciduous forest, *Tree Physiol.*, *20*(11), 725–734.

Hubbard, R. M., B. J. Bond, and M. G. Ryan (1999), Evidence that hydraulic conductance limits photosynthesis in old Pinus ponderosa trees, *Tree Physiol.*, *19*(3), 165–172.

Isaaks, E. H., and R. M. Srivasta (1989), *An Introduction to Applied Geostatistics*, Oxford University Press, New York.

Jarvis, P. G. (1976), Interpretation of variations in leaf water potential and stomatal conductance found in canopies in field, *Philos. Trans. R. Soc. Ser. B-Biological Sciences*, *273*(927), 593–610.

Jarvis, P. G., and K. G. McNaughton (1986), Stomatal control of transpiration-scaling up from leaf to region, *Adv. Ecol. Res.*, *15*, 1–49.

Katul, G., P. Todd, D. Pataki, Z. J. Kabala, and R. Oren (1997), Soil water depletion by oak trees and the influence of root water uptake on the moisture content spatial statistics, *Water Resour. Res.*, *33*(4), 611–623.

Lagergren, F., and A. Lindroth (2002), Transpiration response to soil moisture in pine and spruce trees in Sweden, *Agric. For. Meteorol.*, *112*(2), 67–85.

Landhausser, S. M., U. Silins, V. J. Lieffers, and W. Liu (2003), Response of Populus tremuloides, Populus balsamifera, Betula papyrifera and Picea glauca seedlings to low soil temperature and water-logged soil conditions, *Scandinavian J. For. Res.*, *18*(5), 391–400.

Legendre, P. (1993), Spatial autocorrelation: Trouble or new paradigm?, *Ecology*, *74*(6), 1659–1673.

Legendre, P., and L. Legendre (1998), *Numerical ecology*, 2nd ed., Elsevier, Amsterdam.

Lundblad, M., and A. Lindroth (2002), Stand transpiration and sapflow density in relation to weather, soil moisture and stand characteristics, *Basic Appl. Ecol.*, *3*(3), 229–243.

Mackay, D. S., D. E. Ahl, B. E. Ewers, S. T. Gower, S. N. Burrows, S. Samanta, and K. J. Davis (2002), Effects of aggregated classifications of forest composition on estimates of evapotranspiration in a northern Wisconsin forest, *Global Change Biol.*, *8*(12), 1253–1265.

Mackay, D. S., D. E. Ahl, B. E. Ewers, S. Samanta, S. T. Gower, and S. N. Burrows (2003a), Physiological tradeoffs in the parameterization of a model of canopy transpiration, *Adv. Water Resour.*, *26*(2), 179–194.

Mackay, D. S., S. Samanta, R. R. Nemani, and L. E. Band (2003b), Multiobjective parameter estimation for simulating canopy transpiration in forested watersheds, *J. Hydrol.*, *277*(3–4), 230–247.

Mackay, D. S., B. E. Ewers, B. D. Cook, and K. J. Davis (2007), Environmental drivers of evapotranspiration in a shrub wetland and an upland forest in northern Wisconsin, *Water Resour. Res.*, *43*(3), W03442, doi:10.1029/2006WR005149.

Monteith, J. L. (1965), Evaporation and the environment, paper presented at Proceedings of the 19th Symposium of the Society for Experimental Biology, Cambridge University Press, New York, NY.

Mott, K. A., and D. F. Parkhurst (1991), Stomatal response to humidity in air and helox, *Plant Cell Environ.*, *14*, 509–515.

Oren, R., and D. E. Pataki (2001), Transpiration in response to variation in microclimate and soil moisture in southeastern deciduous forests, *Oecologia*, *127*(4), 549–559.

Oren, R., N. Phillips, G. Katul, B. E. Ewers, and D. E. Pataki (1998), Scaling xylem sap flux and soil water balance and calculating variance: A method for partitioning water flux in forests, *Ann. Des Sci. Forestieres*, *55*(1–2), 191–216.

Oren, R., N. Phillips, B. E. Ewers, D. E. Pataki, and J. P. Megonigal (1999), Sap-flux-scaled transpiration responses to light, vapor pressure deficit, and leaf area reduction in a flooded Taxodium distichum forest, *Tree Physiol.*, *19*(6), 337–347.

Oren, R., J. S. Sperry, B. E. Ewers, D. E. Pataki, N. Phillips, and J. P. Megonigal (2001), Sensitivity of mean canopy stomatal conductance to vapor pressure deficit in a flooded Taxodium distichum L. forest: Hydraulic and non-hydraulic effects, *Oecologia*, *126*(1), 21–29.

Pataki, D. E., R. Oren, and W. K. Smith (2000), Sap flux of co-occurring species in a western subalpine forest during seasonal soil drought, *Ecology*, *81*(9), 2557–2566.

Running, S. W., and J. C. Coughlan (1988), A general-model of forest ecosystem processes for regional applications. 1. Hydrologic balance, canopy gas-exchange and primary production processes, *Ecol. Modell.*, *42*(2), 125–154.

Samanta, S., D. S. Mackay, M. K. Clayton, E. L. Kruger, and B. E. Ewers (2007), Bayesian analysis for uncertainty estimation of a canopy transpiration model, *Water Resour. Res.*, *43*(4), W04424, doi:10.1029/2006WR005028.

Santiago, L. S., G. Goldstein, F. C. Meinzer, and J. H. Fownes (2000), Transpiration and forest structure in relation to soil waterlogging in a Hawaiian montane cloud forest, *Tree Physiol.*, *20*(10), 673–681.

Scanlon, T. M., and J. D. Albertson (2003), Water availability and the spatial complexity of CO2, water, and energy fluxes over a heterogeneous sparse canopy, *J. Hydrometeorol.*, *4*(5), 798–809.

Schafer, K. V. R., R. Oren, and J. D. Tenhunen (2000), The effect of tree height on crown level stomatal conductance, *Plant Cell Environ.*, *23*(4), 365–375.

Sellers, P. J., et al. (1997), Modeling the exchanges of energy, water, and carbon between continents and the atmosphere, *Science*, *275*(5299), 502–509.

Seyfried, M. S., and B. P. Wilcox (1995), Scale and the nature of spatial variability - Field examples having implications for hydrologic modeling, *Water Resour. Res.*, *31*(1), 173–184.

Sperry, J. S., F. R. Adler, G. S. Campbell, and J. P. Comstock (1998), Limitation of plant water use by rhizosphere and xylem conductance: Results from a model, *Plant Cell Environ.*, *21*(4), 347–359.

Spitters, C. J. T., H. Toussaint, and J. Goudriaan (1986), Separating the diffuse and direct component of global radiation and its implications for modeling canopy photosynthesis, 1. Components of incoming radiation, *Agric. For. Meteorol.*, *38*(1–3), 217–229.

Tromp-van Meerveld, H. J., and J. J. McDonnell (2006), On the interrelations between topography, soil depth, soil moisture, transpiration rates and species distribution at the hillslope scale, *Adv. Water Resour.*, *29*(2), 293–310.

Tyree, M. T., and J. S. Sperry (1989), Vulnerability of xylem to cavitation and embolism, *Annu. Rev. Plant Physiol. Plant Mol. Biol.*, *40*, 19–38.

Van Wijk, M. T., S. C. Dekker, W. Bouten, F. C. Bosveld, W. Kohsiek, K. Kramer, and G. M. J. Mohren (2000), Modeling daily gas exchange of a Douglas-fir forest: Comparison of three stomatal conductance models with and without a soil water stress function, *Tree Physiol.*, *20*(2), 115–122.

Vitousek, P. M., H. A. Mooney, J. Lubchenco, and J. M. Melillo (1997), Human domination of Earth's ecosystems, *Science*, *277*(5325), 494–499.

Western, A. W., S. L. Zhou, R. B. Grayson, T. A. McMahon, G. Bloschl, and D. J. Wilson (2004), Spatial correlation of soil moisture in small catchments and its relationship to dominant spatial hydrological processes, *J. Hydrol.*, *286*(1–4), 113–134.

Whitehead, D., and P. G. Jarvis (1981), Coniferous Forests and Plantations, in *Water Deficits and Plant Growth*, edited by T. T. Kowlowski, pp. 49–152, Academic Press, New York.

Whitehead, D., P. G. Jarvis, and R. H. Waring (1984), Stomatal conductance, transpiration, and resistance to water-uptake in a Pinus-sylvestris spacing experiment, *Can. J. For. Res. -Revue Canadienne e Recherche Forestiere*, *14*(5), 692–700.

Wigmosta, M. S., L. W. Vail, and D. P. Lettenmaier (1994), A distributed hydrology-vegetation model for complex terrain, *Water Resour. Res.*, *30*(6), 1665–1679.

Willmott, C. J. (1982), Some comments on the evaluation of model performance, *Bull. Am. Meteorol. Soc.*, *63*(11), 1309–1313.

Wilson, D. J., A. W. Western, R. B. Grayson, A. A. Berg, M. S. Lear, M. Rodell, J. S. Famiglietti, R. A. Woods, and T. A. McMahon (2003), Spatial distribution of soil moisture over 6 and 30 cm depth, Mahurangi river catchment, New Zealand, *J. Hydrol.*, *276*(1–4), 254–274.

Wullschleger, S. D., and A. W. King (2000), Radial variation in sap velocity as a function of stem diameter and sapwood thickness in yellow-poplar trees, *Tree Physiol.*, *20*(8), 511–518.

Zweifel, R., J. P. Bohm, and R. Hasler (2002), Midday stomatal closure in Norway spruce - Reactions in the upper and lower crown, *Tree Physiol.*, *22*(15–16), 1125–1136.

J. D. Adelman and B. E. Ewers, Department of Botany, University of Wyoming, 1000 E. University Avenue, Laramie, WY 82071, USA. (mloranty@buffalo.edu)

E. L. Kruger, Department of Forest and Wildlife Ecology, University of Wisconsin–Madison, 1630 Linden Drive, Madison, WI 53706, USA.

M. M. Loranty and D. S. Mackay, Department of Geography, State University of New York at Buffalo, 105 Wilkeson Quadrangle, Buffalo, NY 14261, USA.